Anal. Bioanal. Electrochem., Vol. 11, No. 5, 2019, 635-646

Analytical & Bioanalytical Electrochemistry

2019 by CEE
www.abechem.com

Full Paper

Surface-Capped SPIONs with EDTA and Structure-Doped with Cobalt Cations: Simple and Fast Preparation by One-Step Electrochemical Synthesis and Characterization

Masoomeh Solgi and Ramin Cheraghali*

Department of Chemistry, Saveh Branch, Islamic Azad University, Saveh, Iran

*Corresponding Author, Tel.: +98-21-44356639; Fax: +98-21-44356639

E-Mail: ramincheraghali@yahoo.com

Received: 5 February 2019 / Received in revised form: 10 April 2019 / Accepted: 21 April 2019 / Published online: 31 May 2019

Abstract- In this paper, EDTA-surface capped and cobalt-cations doped superparamagnetic iron oxide nanoparticles (EDTA/Co-SPIONs) are reported for the first time as a novel surface coated magnetic NPs. An easy and cheap electrochemical strategy is also developed for large-scale fabrication of EDTA/Co-SPIONs. For this aim, a simple cathodic base electrogeneration procedure was established where magnetite nanoparticles formation their surface capping with EDTA and crystal structure doping by Co cations were simultaneously achieved onto the cathode surface. The obtained EDTA/Co-SPIONs powder was analyzed through the structural, elemental and morphological analyses of FT-IR, EDAX, XRD, FE-SEM and DSC-TGA, and their magnetite (i.e. Fe_3O_4) crystal phase was verified by the XRD results, their 10 nm particle size was observed *via* FE-SEM microscopy, their structure doped with 10.69%wt cobalt cations was confirmed though EDAX data, and their surface coat with 10%wt. EDAT was cleared from the thermogravimetric data. VSM measurements proved the superparamagnetic behavior of the EDTA-capped EDTA/Co-IONs powder at the applied fields, where they presented proper saturation magnetization (*Ms*=36.55 emu g^{-1}), negligible remanence (*Mr*=0.86 emu g^{-1}) and low coercivity (*Hci*=9.74Oe). In final, it was concluded that the EDTA-capped Co^{2+} cations doped SPIONs with fine particles exhibit proper magnetic performances for biomedical uses.

Keywords - Iron oxide, Cobalt ion doping, Superparamagnetic particles, Electrochemical synthesis, Biomedical applications

1. INTRODUCTION

As a well-established nanomaterial, superparamagnetic iron oxide nanoparticles (SPIONs) have been widely investigated and applied as the catalysis/photo-catalysis [1,2], energy storage electro-active material [3-8], biomedicine [9-11] and heavy metal removal [12-14]. In the bio-medicine area, SPIONs serves as an ideal platform for improving and upgrading the classical diagnostic imaging and theranostic treatment techniques and also introducing the high impact targeted therapy routs [15,16]. For example, SPIONs are recently studied as the magnetic agents in magnetic resonance imaging (MRI) [17-19], hyperthermia [20-22], drug delivery [23-25], cell labeling [26], bio-sensing [27,28], radioactive therapy [29,30] and tumor therapy [31,32]. These various uses are directly originated from the proper physico-chemical and magnetic characters of SPIONs, which include their uniform particles, facile surface engineering, superparamagnetic nature, controllable size, large magnetic moments, easy synthesis, low toxicity, proper biocompatibility and large surface area [33-35].

Beside chemical techniques developed for the synthesis of SPIONs, it has been reported that the cathodic electrochemical synthesis provides simple and facile route for obtaining the naked and surface capped magnetic nanoparticles [36-42]. Up now, there are various well-established chemical methods for preparing the magnetic nanoparticles (i.e. co-precipitation [43], thermal decomposition [44], hydrothermal [45] and solvothermal [46] procedures) and their functionalization with biocompatible agents. Notably, the fabricated SPIONs should have suitable physic-chemical features like high purity, controlled particle size, single phase, spherical morphology, stability and monodispersity. They also should present the expected magnetic characters such as low coercivity (*Ce*), negligible magnetic remanent (*Mr*) and large saturation magnetization (*Ms*). It should be noted that a major problem involved in the chemical fabrication of SPIONs has been reported to be defining reproducible experimental conditions/or parameters that will produce SPIONs with desired size, narrow size distribution and acceptable magnetic character. For many potential applications of SPIONs, it is necessary that the surface of magnetic core be coated with biocompatible molecules. Up now, various coating layer like as PEI [47], silica [48], PVP [49-51], saccharides [52,53], Au [54], dextran [55,56], EDTA [57,58], amino acids [59,60], chitosan [61], have been deposited onto SPIONs surfaces and their capabilities in the above mentioned field have been studied, and it has been found that the coated biocompatible layers improve the stability of SPIONs and also simplify their further surface functionalization [32,34]. In absence of ad-layer adjustment, the naked MNPs tend to agglomerate as a result of their large surface-to-volume ratio, and their aggregation led to formation of larger magnetic oxide particles, where this type of SPIONs are quickly detected by immune system, and removed from the blood circulation. Furthermore, uncoated/or bare SPIONs be transformed easily into maghemtite (gama-Fe_2O_3) and/or hematite (alpha-Fe_2O_3) in air due to their surface oxidation. This phenomena cause colloidal instability, reducing the saturation magnetization and superparamagnetic ability. Hence, surface coating

adjustment has mentioned to be a key platform to overcome the tendency of SPIONs to aggregation state and limitations related to the magnetic particles utilization in biomedicine/biology [62].

Due to providing the low synthetic temperature, one-step procedure, simplicity and low cost in the fabrication of inorganic nanomaterials with uniform sizes at nano-scale and morphologies (like as particle, plate, rod, tube and sphere), cathodic electrodeposition (CED) has established as a powerful synthetic techniques for preparation of oxide/hydroxide nanostructures [63-67]. In the CED platform, the products are deposited onto the cathode electrode as the result of a two-step electrochemical/chemical mechanism i.e. (*i*) base electro-generation and (*ii*) chemical formation of deposit onto cathode surface [69-70]. In this wok, we report coated surface-capped SPIONs with ethylene diamine tetraacetic acid (EDTA) and crystal structure-doped with cobalt cations prepared through CED route for the first time. The fabricated EDTA coated Co-MNPs were characterized through XRD, FT-IR, FE-SEM, EDS, DSC-TGA and VSM techniques.

2. EXPERIMENTAL PROCEDURE

2.1. Materials

Cobalt (II) nitrate .6H_2O (Sigma Aldrich, 99.5%) iron(III) nitrate .9H_2O (Sigma Aldrich, 99.9%), iron(II) chloride .6H_2O (Sigma Aldrich, 99%) and ethylenediaminetetraacetic acid disodium salt dehydrate (EDTA-Na_2, Sigma Aldrich, 99.9%) were purchased and used as received. The sheets of stainless steel 304 (thickness=5 mm) and graphite plate (thickness=0.5cm) were provided from local companies.

2.2. Fabrication of magnetic samples

The magnetic samples were synthesized *via* cathodic electrochemical synthesis (CES) method i.e. base electrogeneration technique [71-73]. In the CES platform, galvanostatic regime and two electrode electrochemical cell were selected to be used. The cell consisted of the cathode and anode electrodes of stainless steel (304, dimension=5 cm*5 cm) and graphite sheet (dimension=7 cm*7 cm), respectively. The volume of electrochemical cell was 500cc and contain the mixture of 0.5 g $Co(NO_3)_2$ .6H_2O, 2 g $Fe(NO_3)_3$ .9H_2O, 1 g $FeCl_2$.4H_2O and 0.2 g EDTA dissolved deionized water. The optimum current density for deposition of SPIONs surface capped with EDTA onto steel cathode was found to be current of 0.5 A cm^{-2}. The dc 1 A was applied through an external power supply into the electrochemical cell for 10 min and, at the end of deposition time, the dense black film was appeared on to steel cathode. The washing and separation step were followed to obtain dry magnetic powder. First, the cathode was removed from the electrochemical cell and washed several times with ethanol. Then, the deposited black film was collected from the steel surface and the obtained wet powder was

dispersed in 200 cc ethanol solution. At this step, the centrifuging at 4000 rpm for 5 min was carried out to remove the EDTA molecules weekly attached onto the surface of SPIONs. As the final process, the SPIONs were collected from the centrifuged solution by magnet and dried at 80 ^{o}C for 1h.

2.3. Characterization analyses

The particle size and morphological sphere feature of the synthesized SPIONs were determined by field-emission scanning electron microscopy (FE-SEM, Mira 3-XMU with accelerating voltage of 100 kV). The elemental compositions and their weight percentages were also measured through energy dispersive diffraction X-ray (EDS) analyzer linked to the FE-SEM microscope. The powder x-ray diffraction patterns of the fabricated SPIONs and their crystallite size (D) were obtained *via* Phillips PW-1800 XRD instrument. Thermogravimetric behavior of the prepared SPIONs was analyzed through a thermoanalyzer model STA-1500, and their DSC-TG profiles were recorded between 25-500 ^{o}C in N_2 atmosphere. Through a Bruker Vector 22 Fourier transformed infrared spectroscope, the FTIR spectrum of SPIONs was provided at the range of 400 to 4000 cm^{-1}. The magnetic characteristics of the prepared SPIONs were measured in the range of −20000 to 20000 Oe *via* Lake Shore 7400 VSM system.

3. RESULTS AND DISCUSSION

3.1. Crystal structure of SPIONs

Fig. 1 presents XRD pattern of the fabricated EDTA/Co-SPIONs through cathodic deposition method. All the diffractions occurred at the 2theta of 18.08º, 30.77º, 35.74º, 42.85º, 52.68º, 56.91º, 71.52º and 74.07º could be referred to the crystal planes of (111), (220), (311), (400), (422), (511), (440), (533) and (623) respectively. This pattern is well matched with the magnetite crystal phase of iron oxide with cubic spinel structure (i.e. Fe_3O_4, JCPDS 01-088-0315).

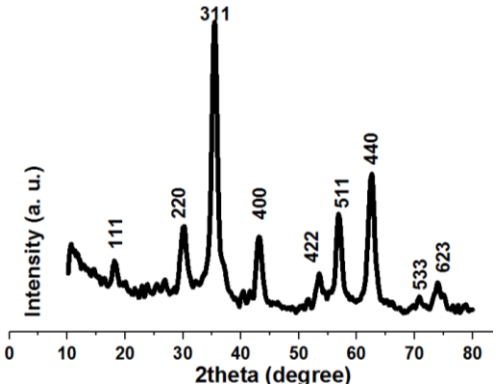

Fig. 1. XRD pattern of the synthesized EDTA/Co-SPIONs powder

As no extra diffraction is seen in Fig. 1, hence it is confirmed that the prepared EDTA/Co-SPIONs has the pure magnetite crystal phase. Using the Scherrer's equation ($D=0.9\lambda/\beta \cos(\theta)$) and diffraction plane of (311), an average crystallite size (D) of 8.4 nm was calculated for the deposited EDTA/Co-SPIONs.

3.2. Surface morphology and particle size of SPIONs

Morphological image and composition data of the synthesized EDTA/Co-SPIONs powder are given in Fig. 2. The FE-SEM images (Fig. 2a) revealed that the prepared SPIONs have particle forms with spherical shapes. Although the observed particles in Fig. 2a are rather agglomerated stats, however they present fine size and uniform distribution. From FE-SEM observation, narrow size distribution and 15 nm in size are easily observable for the prepared Co^{2+} doped SPIONs particles (Fig. 2a).

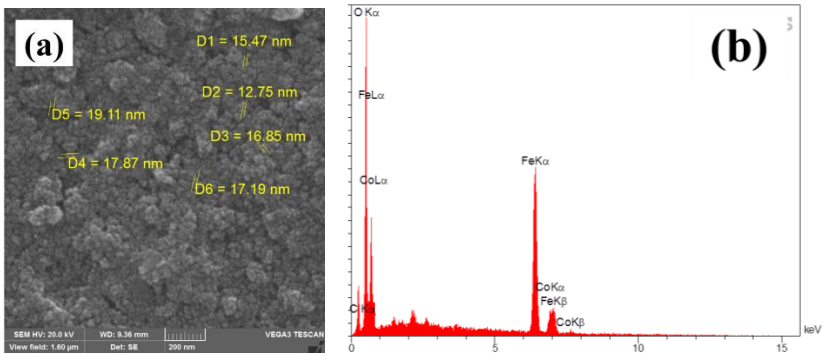

(c)

Elt	W%	A%
O	35.02	42.23
C	17.15	23.18
N	4.30	5.24
Fe	32.84	21.98
Co	10.69	6.37
	100.00	100.00

Fig. 2. (a) FE-SEM image and (b) EDS profile and (c) elemental data of EDTA/Co-SPIONs powder

The EDS profile of the prepared powder is given in Fig. 2b. The elemental detection though Energy-dispersive X-ray spectroscopy (EDS) proved that the prepared SPIONs has comprised by Co, N, O and Fe elements (Fig. 2b). The weight percentages of 4.3%, 17.15 and 35.02 were obtained for C, O and N elements, respectively (Fig. 2c). The presence of these elements (i.e. carbon, oxygen and nitrogen) originates from the EDTA layer capped onto the surface of

SPIONs. The doping of the deposited SPIONs was also confirmed by the EDS profile, where the presence of 10.69%wt. cobalt element with atomic percentage of 6.37% is detected. The iron (32.84%) and oxygen (35.02%) data are also verified the main Fe_3O_4 chemical formula for the deposited SPIONs. Hence, the prepared SPIONs have composition of Fe_3O_4 doped by 10.69% cobalt cations. In final, the 15nm particle size, metal cations doped and EDTA surface capped features of the fabricated SPIONs were specified from FE-SEM images and EDS data.

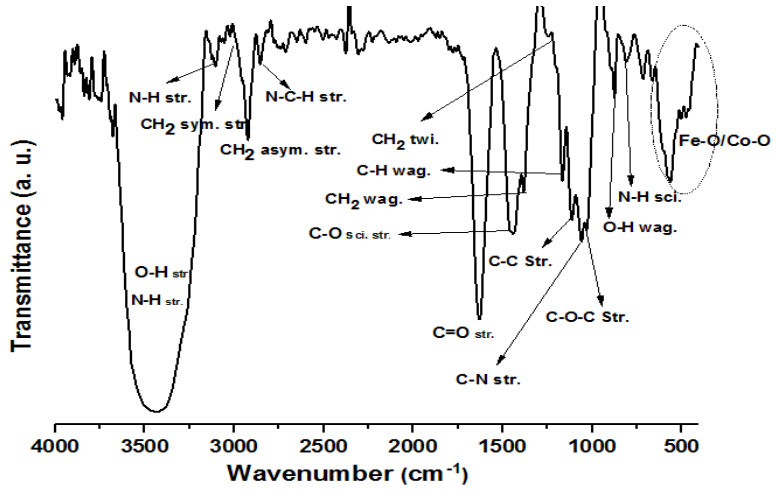

Fig. 3. IR spectrum of the synthesized EDTA-grafted Co^{2+} doped SPIONs

3.3. FT-IR

The synthesized EDTA capped Co-SPIONs sample was also investigated using IR spectroscopy to define its chemical composition. Fig. 3 demonstrated the IR spectrum of the prepared EDTA-grafted Co^{2+} doped SPIONs recorded in the wavenumbers of 400-4000 cm^{-1}. The IR bands at the wavenumbers lower than 700 cm^{-1} could be assigned to the stretching vibrations of metal-oxygen-metal chemical bonds [74,75]. In the IR spectrum of EDTA/Co-SPIONs, two observed IR bands at 579 cm^{-1} and 661 cm^{-1} are related to the splitting of the ν_1 mode vibrations of the Fe^{2+}—O^{2-}/Co^{2+}—O^{2-} chemical bonds [38,41], and a IR band at 433 cm^{-1} is originated from the ν_2 vibration mode of the Fe^{3+}—O^{2-} chemical bonds [39,42]. In the wavenumbers of 750-3500 cm^{-1}, various IR bands are observed, which could be assigned to the following chemical bonds vibrations [55-58]: $\nu_{stretching}$=3400-3450 cm^{-1} for –OH groups, $\nu_{stretching}$=3281 cm^{-1} for N–H bonds, $\nu_{asymmetric\ stretching}$=2985 cm^{-1} for CH_2 groups, $\nu_{symmetric\ stretching}$=2912 cm^{-1} for CH_2 groups, $\nu_{stretching}$=2878 cm^{-1} for N-C–H bonds, $\nu_{stretching}$=1629 cm^{-1} for C=O groups, $\nu_{stretching}$=1479 cm^{-1} for C–O bonds, $\nu_{bending}$=1486 cm^{-1} for C-H bonds, $\nu_{wagging}$=1382 cm^{-1} for CH_3 groups, $\nu_{twisting}$= 1249 cm^{-1} for CH_2 groups, $\nu_{wagging}$=1184 cm^{-1} for C-H bonds, $\nu_{stretching}$=1135 cm^{-1} for C-N bonds, $\nu_{stretching}$=1022 cm^{-1} for C-C bonds,

$\nu_{scissoring}$=1053 cm^{-1} for C-C bonds, $\nu_{stretching}$=1025 cm^{-1} for C-O-C bonds, $\nu_{wagging}$=884 cm^{-1} for O-H bonds and $\nu_{scissoring}$=816 cm^{-1} for N-H bonds. From the above mentioned IR data, it is clearly specified that all the chemical bonds related to EDTA are presented in Fig. 3, confirming the EDTA-capped layer onto the surface of the electrodeposited Co-SPIONs particles.

3.4. Thermo-gravimetric data

Thermal behaviors of the fabricated Co-SPIONs surface coated with EDTA at the temperatures of 25-700 ^oC are given in Fig. 4. In the DSC profile (Fig. 4a), an endothermic peak is seen at T<150 ^oC, which is due to the evaporating the OH^- groups and water molecules lined onto the surface of Co-SPIONs particles [72-74]. A weight loss of 3.98% is measured based on the TG curve for this temperature range (Fig. 4b). After this peak, two successive endothermic behaviors are occurred at the temperature zone of 200 ^oC <T<400 ^oC with peaks at T=210 ^oC and T=265 ^oC (Fig. 4a), which this observation are completely in consist with the reported data for decomposition of EDTA at the temperatures of 200-400 ^oC [57,58,76]. On the TG curve, the main weight loss for this temperature range (i.e. 13.62%wt.) is seen, as donated in Fig. 4b. At the temperatures of 400-700 ^oC, there is one peak on the DSC curve at T=485 ^oC, which could be assigned to the oxidation of magnetite phase into hematite phase [42,52]. For this zone, 1.13%wt. is measured on the TG curve in Fig. 4b. The total weight loss of sample was observed to be 18.73%. These results verified the successful formation of EDTA-capped SPIONs particles.

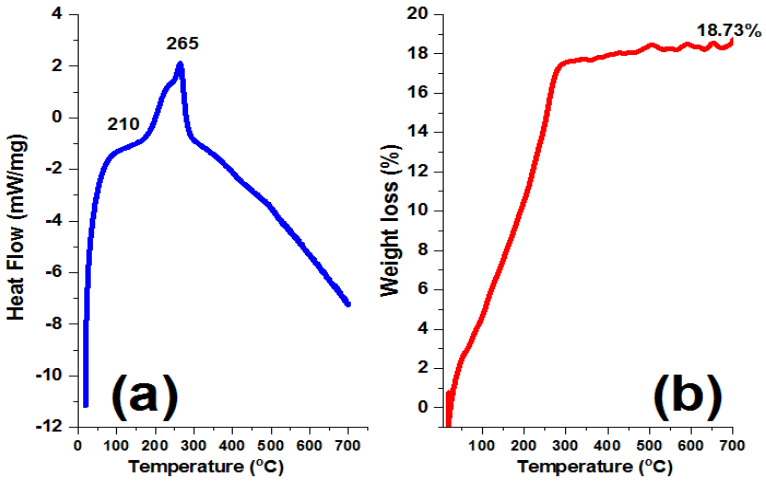

Fig. 4. Thermogravimetric analysis of the prepared EDAT-grafted Co^{2+} doped IONs

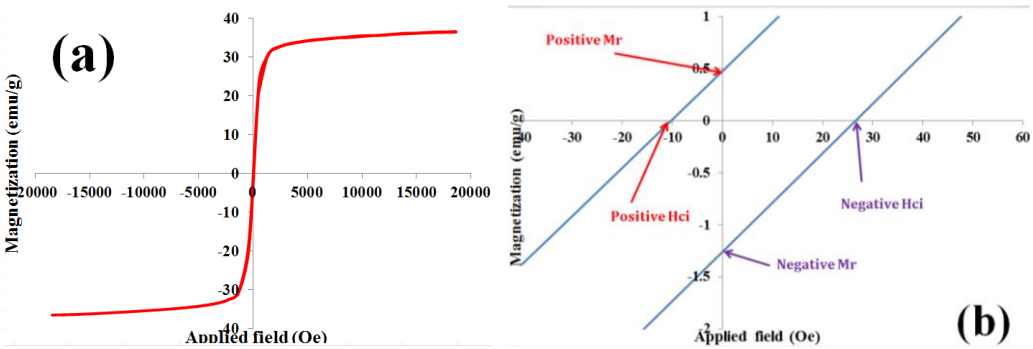

Fig. 5. (a) M-H curves for the fabricated oxide particles, and (b) their hysteresis at Field →0

3.5. Magnetic evaluation

The magnetization data of the prepared EDTA-capped Co^{2+}-doped SPIONs nanoparticles SPIONs were recorded at the applied fields in the rage of -20000Oe to +20000Oe, and the VSM curve are plotted in Fig. 5a. Furthermore, the magnetization profile of sample was provided at the conditions of applied field→0 (Fig. 5b), and the remanence (*Mr*) and coercivity (*Hci*) of sample were determined using this curve. From Fig. 5a, it is verified that the prepared nanoparticles show superparamagnetic properties due to the absence of any hysteresis loop at the applied fields and also S shape of their VSM curve. The obtained data from Figs. 5a and b including *Ms*, *Mr* and *Hci* are listed in Table 1. For comparison, the magnetic data reported for the naked IONs and Co-doped IONs are also provided from Refs. [16]. The prepared EDTA-capped Co^{2+}-doped SPIONs exhibited *Ms*, *Mr* and *Hci* values of 36.55 emu/g, 0.86 emu/g and 9.74 Oe, respectively. These data specified the superparamagnetic nature of the prepared SPIONs, which is comparable with those reported for the naked SPIONs.

Table 1. Magnetic data of the Co-doped and undoped SPIONs

Sample name	Ms (emu/g)	Coercivity (Hci) Oe	Positive (Hci) Oe	Negative (Hci) Oe	Negative Mr (emu/g)	Positive Mr (emu/g)	Retentivity Mr (emu/g)
Naked SPIONs [a]	72.96	14.6	-41.87	-12.66	0.83	2.73	0.95
EDTA/Co-SPIONs	36.55	9.74	-10.71	24.65	-1.24	-0.48	0.86

[a] provided from Ref. [4]

Compared to the naked SPIONs, the EDTA-capped SPIONs particles exhibited lower *Ms* value (Table 1), which is due the non-magnetic EDTA layer and also the reduced magnetite

weight in the prepared SPIONs. However, the EDTA-grafted Co^{2+}-doped IONs exhibited lower remanence and coercivity (*Mr*=0.86 emu/g and coercivity (*Hci*=9.74 Oe) as compared to the naked IONs (*Mr*=0.95 emu/g and coercivity (*Hci*=14.6 Oe), which it was found that the superparamagnetic behavior of SPIONs is improved as results of cobalt cations doping into the SPIONs crystal structure and EDTA capping onto their particle surfaces.

4. CONCLUSION

In summary, a fast and very simple method was proposed and verified for the preparation of superparamagnetic iron oxide nanoparticles surface capped with EDTA layer and crystal structure doped with Co^{2+} cations. The FE-SEM observations and EDAX data revealed that the electro-deposited SPIONs are doped with about 10.69% wt. cobalt cations with 20nm in particle size. The magnetite crystal structure and EDTA layer onto the SPIONs were also confirmed through XRD and FT-IR analyses. The prepared Co-SPIONs exhibited superparamagnetic nature with showing the saturation magnetization, remanence and coercivity of of 36.55 emu g^{-1}, 0.86 emu g^{-1} and 9.74 Oe, respectively. The results of this work verified the primary suitability of EDT/Co-SPIONs for biomedical applications.

REFERENCES

[1] S. Chi, C. Ji, S. Sun, H. Jiang, R. Qu, and C. Sun, Ind. Eng. Chem. Res. 55 (2016) 12060.
[2] M. Amir, S. Güner, A. Yıldız, and A. Baykal, J. Magn. Magn. Mater. 421 (2017) 462.
[3] M. Aghazadeh, I. Karimzadeh, and M. R. Ganjali, J. Mater. Sci.: Mater. Electron. 28 (2017) 13532.
[4] M. Aghazadeh, and M. R. Ganjali, J. Mater. Sci. 53 (2018) 295.
[5] M. Aghazadeh, and M. R. Ganjali, Ceram. Int. 44 (2018) 520.
[6] M. Aghazadeh, I. Karimzadeh, M. R. Ganjali, and A. Behzad, J. Mater. Sci.: Mater. Electron. 28 (2017) 18121.
[7] M. Aghazadeh, I. Karimzadeh, and M. R. Ganjali, Mater. Lett. 209 (2017) 450.
[8] M. Aghazadeh, and M. R. Ganjali, J. Mater. Sci.: Mater. Electron. 29 (2018) 2291.
[9] E. Mostaghasi, A. Zarepour, and A. Zarrabi, J. Taiwan Institute Chem. Engin. 82 (2018) 33.
[10] N. V. Srikanth Vallabani, and S. Singh, 3 Biotech 8 (2018) 279.
[11] X. Liu, S. Lu, D. Liu, L. Zhang, L. Zhang, X. Yu, and R. Liu, Brain Res. 1707 (2019) 141.
[12] M. Aghazadeh, I. Karimzadeh, and M. R. Ganjali, Curr. Nanosci. 15 (2019) 169.
[13] A. Kumar, G. Sharm, M. Naushad, and S. Thakur, Chem. Eng. J. 280 (2015) 175.
[14] Y. Zhang, W. Yan, L. Xu, X. Guo, L. Cui, L. Gao, Q. Wei, and B. Du, J. Mol. Liquid. 191 (2014) 177.

[15] H. Fakhimikabir, M.B. Tavakoli, A. Zarrabi, A. Amouheidari, and S. Rahgozar, J. Photochem. Photobiol. B 182 (2018) 71.
[16] C. Scialabba, R. Puleio, D. Peddis, G. Varvaro, P. Calandra, G. Cassata, L. Cicero, M. Licciardi, and G. Giammona, Nano Res. 10 (2017) 3212.
[17] K. Wang, L. Li, X. Xu, L. Lu, J. Wang, S. Wang, Y. Wang, Z. Jin, J.Z. Zhang, and Y. Jiang, ACS Appl. Mater. Interfaces 11 (2019) 10452.
[18] X. He, X. Shen, D. Li, Y. Liu, K. Jia, and X. Liu, ACS Appl. Bio Mater. 1 (2018) 520.
[19] A. M. Demin, A. G. Pershina, A. S. Minin, A. V. Mekhaev, V. V. Ivanov, S. P. Lezhava, A. A. Zakharova, I. V. Byzov, M. A. Uimin, V. P. Krasnov, and L. M. Ogorodova, Langmuir 34 (2018) 3449.
[20] X. Wang, J. Zhang, H. Zhang, X. Yang, and Y. Huang, J. Biomater. Sci. 29 (2018) 181.
[21] G. Kandasamy, A. Sudame, P. Bhati, A. Chakrabarty, and D. Maity, J. Molecular Liquids 256 (2018) 224.
[22] L. Storozhuk, and N. Iukhymenko, Appl. Nanosci. (2019). doi:10.1007/s13204-018-0777-x.
[23] N. Thi Hanh, N. T. Xuyen, T. T. Thanh Thuy, Vietnam J. Chem. 56 (2018) 642.
[24] M. G. Adimoolam, N. Amreddy, M. R. Nalam, and M. V. Sunkara, J. Magn. Magn. Mater. 448 (2018) 199.
[25] D. Li, M. Deng, Z. Yu, W. Liu, G. Zhou, W. Li, X. Wang, D. P. Yang, and W. Zhang, ACS Biomater. Sci. Eng. 4 (2018) 2143.
[26] P. Naserzadeh, A. Ashrafi Hafez, M. Abdorahim, M. A. Abdollahifar, H. Peirovi, A. Simchi, and K. Ashtari, Biomed. Pharmacotherapy 108 (2018) 1244.
[27] M. Hosseini, M. Aghazadeh, and M. R. Ganjali, New J. Chem. 41 (2017) 12678.
[28] S. A. Adams, J. L. Hauser, A. C. Allen, K. P. Lindquist, A. P. Ramirez, S. Oliver, and J. Z. Zhang, ACS Appl. Nano Mater. 1 (2018) 1406.
[29] S. Klein, J. Hübner, C. Menter, L. V. R. Distel, W. Neuhuber, and C. Kryschi, Appl. Sci. 9 (2019) 15.
[30] X. Zhang, Z. Liu, Z. Lou, F. Chen, S. Chang, and Y. Miao, Artificial Cells 46 (2018) 975.
[31] S. Al-Musawi, M. Jawad Kadhim, and N. Khazal Kadhim, Hindi J. Pharm. Sci. Res. 10 (2018) 749.
[32] R. Mout, D. F. Moyano, S. Rana, and V. M. Rotello, Chem. Soc. Rev. 41 (2012) 2539.
[33] K. Turcheniuk, A. V. Tarasevych, V. P. Kukhar, R. Boukherrouba, and S. Szunerits, Nanoscale 5 (2013) 10729.
[34] N. Erathodiyil, and J. Y. Ying, Acc. Chem. Res. 44 (2011) 925.
[35] M. Aghazadeh, M. R. Ganjali, and P. Norouzi, Mater. Res. Express 3 (2016) 055013.
[36] M. Aghazadeh, I. Karimzadeh, and M. R. Ganjali, J. Mater. Sci.: Mater. Electron. 28 (2017) 19061.
[37] M. Aghazadeh, and I. Karimzadeh, Mater. Res. Express 4 (2017) 105505.

[38] M. Aghazadeh, I. Karimzadeh, and M. R. Ganjali, J. Mater. Sci.: Mater. Electron. 29 (2018) 5163.
[39] M. Aghazadeh, and M. R. Ganjali, J. Mater. Sci.: Mater. Electron. 29 (2018) 4981.
[40] M. Aghazadeh, J. Mater. Sci.: Mater. Electron. 28 (2017) 18755.
[41] M. Aghazadeh, I. Karimzadeh, and M. R. Ganjali, J. Electron. Mater. 47 (2018) 3026.
[42] M. Aghazadeh, I. Karimzadeh, and M. R. Ganjali, Phys. Status Solidi A 214 (2017) 1700365.
[43] S. Vidawati, S. Barbosa, P. Taboada, E. Villar, A. Topete, and B. V. Mosquera, Adv. Biol. Chem. 8 (2018) 91.
[44] S. Klein, L. M. S. Stiegler, C. Harreiss, L. V. R. Distel, W. Neuhuber, E. Spiecker, A. Hirsch, and C. Kryschi, ACS Appl. Bio Mater. 1 (2018) 2002.
[45] H. Köçkar, O. Karaagac, and F. Özel, J. Magn. Magn. Mater. 474 (2019) 332.
[46] A. Yan, X. Liu, G. Qiu, H. Wu, R. Yi, N. Zhang, and J. Xu, J. Alloys Compd. 458 (2008) 487.
[47] I. Karimzadeh, M. Aghazadeh, M. R. Ganjali, and T. Dourudi, Curr. Nanosci. 13 (2017) 167.
[48] G. S. An, D. H. Chae, J. U. Hur, A. H. Oh, H. H. Choi, S. C. Choi, Y. S. Oh, and Y. G. Jung, Ceram. Int. 44 (2018) 18791.
[49] M. Aghazadeh, Anal. Bioanal. Electrochem. 10 (2018) 508.
[50] M. Aghazadeh, I. Karimzadeh, and M. R. Ganjali, Mater. Lett. 228 (2018) 137.
[51] I. Karimzadeh, M. Aghazadeh, M. R. Ganjali, P. Norouzi, S. Shirvani-Arani, T. Doroudi, P. H. kolivand, S. A. Marashi, and D. Gharailou, Mater. Lett. 179 (2016) 5.
[52] M. Aghazadeh, I. Karimzadeh, M. R. Ganjali, and M. M. Morad, Mater. Lett. 196 (2017) 392.
[53] I. Karimzadeh, M. Aghazadeh, M. R. Ganjali, P. Norouzi, T. Doroudi, and P. H. Kolivand, Mater. Lett. 189 (2017) 290.
[54] N. Singh, J. Nayak, S. K. Sahoo, and R. Kumar, Mater. Sci. Eng. C 100 (2019) 453.
[55] M. Aghazadeh, Anal. Bioanal. Electrochem. 11 (2019) 362.
[56] Q. Wu, T. Miao, T. Feng, C. Yang, Y. Guo, and H. Li, Mol. Medic. Report. 18 (2018) 564.
[57] A. G. Magdalena, I. M. B. Silva, R. F. C. Marques, A. R. F. Pipi, and M. Jafelicci, J. Phys. Chem. Solids 113 (2018) 5.
[58] E. Shah, P. Upadhyay, M. Singh, M. Shoab Mansuri, R. Begum, N. Shethd, and H. P. Soni, New J. Chem. 40 (2016) 9507.
[59] M. Aghazadeh, I. Karimzadeh, M. R. Ganjali, D. Gharailou, and P. Kolivand, Curr. Nanosci. 13 (2017) 274.
[60] M. Aghazadeh, I. Karimzadeh, A. Ahmadi, M. R. Ganjali, and P. Norouzi, J. Mater. Sci.: Mater. Electron. 29 (2018) 14378.

[61] M. Aghazadeh, and I. Karimzadeh, Curr. Nanosci. 14 (2018) 42.
[62] G. S. Demirera, A. C. Okur, and S. Kizilel, J. Mater. Chem. B 3 (2015) 7831.
[63] M. Aghazadeh, and M. R. Ganjali, J. Mater. Sci.: Mater. Electron. 28 (2017) 8144.
[64] M. Aghazadeh, and M. R. Ganjali, J. Mater. Sci.: Mater. Electron. 28 (2017) 11406.
[65] M. Aghazadeh, and S. Dalvand, J. Electrochem. Soc. 161 (2014) D18.
[66] M. Aghazadeh, M. Ghaemi, A. N. Golikand, and A. Ahmadi, Mater. Lett. 65 (2011) 2545.
[67] M. Aghazadeh, T. Yousefi, and M. Ghaemi, J. Rare Earths 30 (2012) 236.
[68] M. Aghazadeh, A. N. Golikand, M. Ghaemi, and T. Yousefi, Mater. Lett. 65 (2011) 1466.
[69] M. Aghazadeh, M. Hosseinifard, B. Sabour, and S. Dalvand, Appl. Surf. Sci. 287 (2013) 187.
[70] M. Aghazadeh, Anal. Bioanal. Electrochem. 11 (2019) 211.
[71] M. Aghazadeh, A. Rashidi, and M. R. Ganjali, Electron. Mater. Lett. 14 (2018) 37.
[72] M. Aghazadeh, I. Karimzadeh, A. Ahmadi, and M. R. Ganjali, J. Mater. Sci.: Mater. Electron. 29 (2018) 14567.
[73] M. Aghazadeh, M. G. Maragheh, M. R. Ganjali, and P. Norouzi, Inorg. Nano-Metal Chem. 27 (2017) 1085.
[74] M. Aghazadeh, J. Mater. Sci.: Mater. Electron. 28 (2017) 3108.
[75] M. Aghazadeh, Mater. Lett. 211 (2018) 225.
[76] P. Norouzi, H. Haji-Hashemi, N. Ghaheri, and B. Larijani, Anal. Bioanal. Electrochem. 10 (2018) 478.